Archives of Materials Science and Engineering

Volume 111
Issue 2
October 2021
Pages 49-65

International Scientific Journal published monthly by the World Academy of Materials and Manufacturing Engineering

DOI: 10.5604/01.3001.0015.5805

Free vibration analysis of imperfect functionally graded sandwich plates: analytical and experimental investigation

E.K. Njim [a], S.H. Bakhy [a], M. Al-Waily [b,*]

[a] Mechanical Engineering Department, University of Technology, Baghdad, Iraq

[b] Department of Mechanical Engineering, Faculty of Engineering, University of Kufa, Kufa, Iraq

* Corresponding e-mail address: muhanedl.alwaeli@uokufa.edu.iq

ORCID identifier: https://orcid.org/0000-0002-7630-1980 (M.A-.W.)

ABSTRACT

Purpose: This paper develops a new analytical solution to conduct the free vibration analysis of porous functionally graded (FG) sandwich plates based on classical plate theory (CPT). The sandwich plate made of the FGM core consists of one porous metal that had not previously been taken into account in vibration analysis and two homogenous skins.

Design/methodology/approach: The analytical formulations were generated based on the classical plate theory (CPT). According to the power law, the material properties of FG plates are expected to vary along the thickness direction of the constituents.

Findings: The results show that the porosity parameter and the power gradient parameter significantly influence vibration characteristics. It is found that there is an acceptable error between the analytical and numerical solutions with a maximum discrepancy of 0.576 % at a slenderness ratio (a/h =100), while the maximum error percentage between the analytical and experimental results was found not exceeding 15%.

Research limitations/implications: The accuracy of analytical solutions is verified by the adaptive finite elements method (FEM) with commercial ANSYS 2020 R2 software.

Practical implications: Free vibration experiments on 3D-printed FGM plates bonded with two thin solid face sheets at the top and bottom surfaces were conducted.

Originality/value: The novel sandwich plate consists of one porous polymer core and two homogenous skins which can be widely applied in various fields of aircraft structures, biomedical engineering, and defense technology. This paper presents an analytical and experimental study to investigate the free vibration problem of a functionally graded simply supported rectangular sandwich plate with porosities. The objective of the current work is to examine the effects of some key parameters, such as porous ratio, power-law index, and slenderness ratio, on the natural frequencies and damping characteristics.

Keywords: Functionally graded materials, Sandwich plate, Porous metal, Frequency analysis, Finite element methods (FEM)

Reference to this paper should be given in the following way:

E.K. Njim, S.H. Bakhy, M. Al-Waily, Free vibration analysis of imperfect functionally graded sandwich plates: analytical and experimental investigation, Archives of Materials Science and Engineering 111/2 (2021) 49-65. DOI: https://doi.org/10.5604/01.3001.0015.5805

METHODOLOGY OF RESEARCH, ANALYSIS AND MODELLING

1. Introduction

In a few decades, functionally graded materials (FGMs) have become extensively used as sophisticated engineering materials in a wide range of applications, including workpiece materials, space systems, energy, dental implants, and prostheses [1]. Using a functionally graded porous core material (FGPMs) in sandwich structures increases because of its features in reducing residual and thermal stresses generated between the core and the skins compared to conventional sandwich structures. Therefore, they are utilized in the aerospace, defense, marine, and automotive industries. The functionally graded material has the function of designing with the change of the material's position itself compared with the homogeneous core material. It has the potential to become a more effective core material due to its excellent characteristics [2]. Because of their importance in biomaterial engineering, functionally graded materials with porosity, and microstructure gradients are being developed [3].

In general, porous functionally graded materials, FGPMs, are generated by changing the porosity concentration or pore volume in either a continuous or gradual process [4,5]. In the past few years, substantial interest has been undertaken in understanding the dynamic characteristics of the functionally graded sandwich plate. Zenkour [6] studied the dynamic response of FG sandwiched between thick rectangular plates using a quasi-3D shear deformation theory. Arefi and Najafitabar [7] investigated free vibration and buckling analyses of FGM sandwich beams with uniform hardcore and FG skins. Sciuva and Sorrenti [8] investigated the vibration response and buckling loads of FG sandwich plates under various symmetrical loadings using the modified Refined Zigzag theory. Amirpour et al. [9] explored the free vibration characterization of simply supported 3D printed polymeric functionally graded (FG) plates using Higher-Order Shear Deformation Theory and finite element techniques. Wattanasakulpong and Ungbhakorn [10] investigated the linear and nonlinear vibrations of elastically constrained edges of FGM beams with pores.

Wattanasakulpong and Chaikittiratana [11] examined the free vibration of Timoshenko beams with porosities, taking into account the uneven distribution of porosities in the model. Muc and Flis [12] used both first-order transverse shear deformation and classical (CPT) theory to examine the free vibrations of thin and substantially thick porous FGM plates with different boundary conditions. They validated the results by employing the Rayleigh-Ritz methods. Xie et al. [13] developed a theoretical method for the free vibration analysis of FGM plates with porosity variation depending on the energy measurements. The morphology of the porosity distributions is also taken into account. Hayat and Meriem [14] conducted dynamic analysis on FG plates with pores made of a combination of metal and ceramic enclosed in an elastic medium. Zhang et al. [15] investigated the mechanical performance of functionally graded structures and the topological design of porous materials.

Mostefa and Slimane [16] introduced an exact solution to examine the effects of porosity distribution and the material volume fraction on the dynamic behavior of the FGM sandwich plate under various boundary conditions. Singh and Harsha [17] analysed the free vibration characteristics of the FGM sandwich plate with 3 types of porosity arrangement. Kumar et al. [18] studied the free vibration analysis of tapered FGM plates mounted on an elastic foundation according to first-order shear deformation theory. Moreover, Khan et al. [19] extensively studied the modal analysis of composite sandwich materials, containing Nano polyurethane foam cores. Kaddari et al. [20] investigated static and dynamic analysis of a porous FG plate resting on an elastic foundation using a new quasi three-dimensional model. Li et al. [21] investigated the dynamic response of a porous FG sandwich plate having a core reinforced with graphene nanoparticles. Relying on the modified Fourier-Ritz approach, Xue et al. [22] developed a damped free vibration analysis of FG sandwich panels with porosities. Abderrahmane et al. [23] studied the effects of boundary conditions on the dynamic behavior of functionally graded sandwich plates with auxetic 3D lattice metamaterials cores. Li et al. [24] investigated free vibration of FG sandwich plates using FEA and experimental methods.

Many researchers have also investigated the effect of thermal conditions on sandwich plates. Brischetto [25] presented an analysis of a composite laminated shell under the hygrothermo-elastic effect. Therefore, the effect of thermal and hygroscopic loads on the strain and stress was presented by using analytical techniques. Then, Garg and Chalak [26], presented a review of the hygrothermal condition's effect on the laminated sandwich plate structure. There, the review predicted the mechanical behavior of the laminated structure under hygrothermal effects such as vibration and buckling behavior.

Garg and Chalak, [27], investigated the effect of the hygro-thermomechanical-conditions on the stress analysis for skew and non-skew laminated sandwich structure. The theory of higher-order zigzag was used to analyze the mechanical behavior of composite laminate sandwich plates. In addition, numerical technique, by using the finite element with using the Nine-noded isoparametric element, used to analyze the results were calculated.

After this, Krishna and Chalak, [28], presented the analysis of the mechanical behavior of composite sandwich plate structure under thermal effect. There, the analysis included used for the numerical technique to calculate the mechanical behavior for the plate under various thermal effects. In addition, the investigation included calculates various mechanical behavior for plates with different sandwich plate parameters, with thermal effect. Kumar et al., [29], analyzed the non-linear behavior for stress and deflection of the laminated sandwich plate with the effect of the cutout. So, the cutout investigation was the elliptical shape and the stress and deflection for plate structure analysis under hygro-thermal with various transverse loadings.

Garg et al. [30] conducted a comparative study of sandwich functionally graded beams made up of power-law and exponential and sigmoidal laws under free vibration conditions. The study has been carried out using the higher-order zigzag theory. The present formulation incorporates transverse normal stress and hence is more efficient. Also, the present formulation satisfies zero transverse shear stress conditions at the top and bottom surfaces of the beam.

Hirane et al. [31] developed a layerwise finite element model for static and free vibration analysis of FGM sandwich plates using higher-order theory. Vinh and Tounsi [32] investigated the behavior of the spatial variation of the nonlocal parameter on the free vibration of simply supported FG sandwich nanoplates. It is revealed that there is an essential effect of the nonlocal parameters in the free vibration of functionally graded sandwich nanoplates.

Vinh and Huy [33] introduced the FEM model based on a new hyperbolic shear deformation theory to investigate the mechanical behavior of the PFGM sandwich plates. Vinh [34] introduced a comprehensive investigation of bi-directional FG sandwich plates using higher-order shear deformation theory and the FEM method to study the free vibration and buckling behaviors. The results show that the variation of the material ingredients and properties, the boundary conditions, and the thickness ratio of layers play significant roles in the stability of bi-directional FG sandwich plates.

The present study aims to analyse the free vibration characteristics of the functionally graded porous materials structure. The plate material characteristics are to vary smoothly within the thickness direction only according to the power-law distribution. The mathematical model for the free vibration of a simply supported rectangular FG sandwich plate is derived based on the CPT to find the natural frequency according to various FGM parameters. The FGM parameters are porous index, porosity ratio, aspect, and slenderness ratios. The experimental tests were conducted using a portable digital vibrometer system to calculate the first natural frequency of the well-designed and manufactured 3D printed polymer FGM sandwich plate samples. Along with experimental methods, numerical investigation using the finite element method is extensively used to check the accuracy of both the proposed analytical and numerical solutions. The numerical results are reported for various parameters.

2. Mathematical formulation of FGM

Although there are many studies of the FG structure that have investigated the vibrational behaviour of FG plate, assumed metal-ceramic FGM in their assessment due to their high mechanical strength, and polymeric or metallic polymers are less discussed. Thus, if the volume fraction of the upper surface of the FG plate is V_U and that of the lower surface is, V_L then by introducing a power-law distribution of the constituents across the plate thickness, The volume fraction of the upper constituent may be assumed to be of the form [24],

$$V_U(z) = \left(\frac{z+\frac{h}{2}}{h}\right)^r \tag{1}$$

The corresponding volume fraction of the mixture can be given by,

$$V_U(z) + V_L(z) = 1 \tag{2}$$

Here z denotes normal coordinates to the middle surface of the plate and varies from $-h/2$ to $h/2$, h is the thickness of the FG plate, r denotes a power-law variation index ($r \leq 0 \leq \infty$) which describes material property variation in thickness. The effective material properties of the FG plate can be formulated as,

$$P(z) = (P_L - P_U)\left(\frac{z+\frac{h}{2}}{h}\right)^r + P_U \tag{3}$$

In Equation (3), P_U and P_L are corresponding material properties of the upper and the lower constituents of the FG plate, respectively. In the current investigation, it considered that the plate consists only of one metal with density changes across the thickness, and the suggested rule of the volume fraction can be expressed as,

$$V_p(z) = V_m - \gamma . V_m \left(\frac{z}{h} + \frac{1}{2}\right)^r \tag{4}$$

For $r = 0$, $V_p(z) = V_m - \gamma V_m$, while for; $r = \infty$, $V_p = V_m = 1$, where V_p is the total volume of porous metal, V_m is the volume of core metal, and γ is the porosity parameter. Consequently, the proposed mechanical properties of the FGM porous metal can be represented as,

$$P(z) = P_m - \gamma . P_m \left(\frac{z}{h} + \frac{1}{2}\right)^r \tag{5}$$

Here P_m is the value of the material properties of metal of the FG plate. Thus for the homogenous plate ($\gamma = 0$), while for imperfect FG plate ($\gamma < 1$).

3. Suggested mathematical modelling for sandwich plate with FGM porous core

By using the classical plate theory (CPT), the differential equation of FG plates across the plate thickness at a distance z away from the middle surface is given by: [35,36],

$$\frac{\partial^2 M_{xx}}{\partial x^2} - 2\frac{\partial^2 M_{xy}}{\partial x.\partial y} + \frac{\partial^2 M_{yy}}{\partial y^2} = I_0 \frac{\partial^2 w}{\partial t^2} \tag{6}$$

Rearranging equation 6 in terms of flexural rigidity and bending equation, we can obtain the equation of equilibrium in terms of deflections (w) of the plate as,

$$D\left(\frac{\partial^4 w}{\partial x^4} + 2\frac{\partial^4 w}{\partial x^2 . \partial y^2} + \frac{\partial^4 w}{\partial y^4}\right) + I_0 \frac{\partial^2 w}{\partial t^2} = 0 \tag{7}$$

Where, $D = \frac{Eh^3}{12(1-\mu^2)}$, is the flexural rigidity of the plate, I_o is the inertial coefficient of the plate, E is Young's modulus and μ is the Poisson's ratio. Consider a simply supported sandwich plate of length a and width b, comprising mainly from the single-phase core metal having an even distribution of porosities (Beta) while the top and bottom plate surfaces, using same isotropic and geometrical properties as shown in Figure 1. The material properties of the upper and lower face sheets are assumed to be identical; hence, the mechanical properties $E_{UP} = E_{LP}$, $\upsilon_{UP} = \upsilon_{LP=}\upsilon$ and the mass density $\rho_{UP} = \rho_{LP}$. For the imperfect FGM plate, Young's modulus (E) and material density (ρ) are taken to vary along the thickness direction, except for Poisson's ratio (μ) will assume to be constant for simplicity [15]. Hence, the elasticity modulus E and material density ρ of porous FG core layer can be expressed, respectively, as,

$$E(z) = E_m - \gamma . E_m \left(\frac{z}{h} + \frac{1}{2}\right)^r \tag{8}$$

$$\rho(z) = \rho_m - \gamma . \rho_m \left(\frac{z}{h} + \frac{1}{2}\right)^r \tag{9}$$

By incorporating Equations (8) and (9) into Equation (7), and assuming the thickness of upper and lower skins are equal ($h_{UP}=h_{LP}$), the general form of both effective flexural rigidity D_{SP} and inertia I_o of the sandwich plate can be expressed as follows,

$$D_{sp} = \int_{-h/2}^{h/2} E(z).z^2\,dz \tag{10}$$

$$D_{sp} = \left(\begin{array}{c} \frac{E_m h^3}{12(1-\mu^2)} - \frac{\gamma E_m h^3}{(1-\mu^2)}\left(\frac{1}{(r+3)} - \frac{1}{(r+2)} + \frac{1}{4(r+1)}\right) \\ + \frac{E_{UP}}{(1-\mu_{UP}^2)}\left(\frac{2(\frac{h}{2}+h_{UP})^3}{3} - \frac{h^3}{12}\right) \end{array}\right) \tag{11}$$

$$I_o = \int_{-h/2}^{h/2} \rho(z)\,dz \tag{12}$$

$$I_{SP} = \rho_m h\left(1 - \frac{\gamma}{(r+1)}\right) + 2\rho h_{UP} \tag{13}$$

$$D_{SP}\left(\frac{\partial^4 w}{\partial x^4} + 2\frac{\partial^4 w}{\partial x^2 . \partial y^2} + \frac{\partial^4 w}{\partial y^4}\right) + I_0 \frac{\partial^2 w}{\partial t^2} = 0$$

Or,

$$\left(\begin{array}{c} D_{SP}\left(\frac{\partial^4 w}{\partial x^4} + 2\frac{\partial^4 w}{\partial x^2 . \partial y^2} + \frac{\partial^4 w}{\partial y^4}\right) + \\ \left(\rho_m h\left(1 - \frac{\gamma}{(r+1)}\right) + 2\rho h_{UP}\right)\frac{\partial^2 w}{\partial t^2} \end{array}\right) = 0 \tag{14}$$

The separation of the variables method can be used to treat Equation (14) by assuming the function of deflection as, [37,38],

$$w(x,y,t) = w(x,y) \times w(t) \tag{15}$$

Where $w(t)$ is the deflection function of the plate concerning time, and $w(x,y)$ is the deflection of the plate can be represented as a function of (x) and (y) in the following form [39-41],

$$w(x,y) = sin\frac{m\pi x}{a} sin\frac{n\pi y}{b} \qquad m,n = 1,2,3 \ldots \tag{16}$$

Then, by substation Equation 14 into Equation16, and apply the boundary conditions for simply supported plate (w=0 and M=0; for all four edges) hence, the general equation of motion for FGM rectangular plate in terms of rigidities is obtained as,

$$\left(\begin{array}{c} D_{SP}\left(\left(\frac{\pi}{a}\right)^4 + 2\times\left(\frac{\pi}{a}\right)^2\left(\frac{\pi}{b}\right)^2 + \left(\frac{\pi}{b}\right)^4\right)w(t) + \\ \left(\rho_m h\left\{1 - \frac{\gamma}{(r+1)}\right\} + 2\rho h_{UP}\right)\frac{\partial^2 w}{\partial t^2} \end{array}\right) = 0 \tag{17}$$

A second-order ordinary differential Equation (17) is comparable to a general equation of motion for an undamped vibration structure, which is presented in [42],

$$\omega_{mn}^2 . w(t) + \frac{\partial^2 w(t)}{\partial t^2} = 0 \tag{18}$$

However, the suggested equation of natural frequency (ω) for the rectangular FGM sandwich plate with porosity distribution is as follows,

$$\omega = \left(\frac{D_{SP}\left(\left(\frac{\pi}{a}\right)^4 + 2\left(\frac{\pi}{a}\right)^2\left(\frac{\pi}{b}\right)^2 + \left(\frac{\pi}{b}\right)^4\right)}{\left(\rho_m h\left\{1 - \frac{\gamma}{(k+1)}\right\} + 2\rho h_{UP}\right)} \right)^{1/2} \tag{19}$$

a)

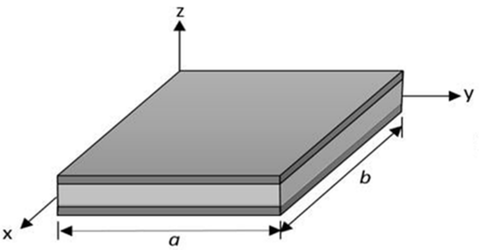

b)

c)

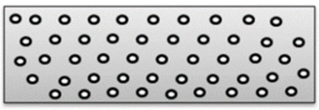

Fig. 1. FGM porous sandwich plate with even distribution of porosities; a) plate modelling, b) thickness section for plate, c) porous section for plate

4. Finite Element Modelling

In most cases, verify the analytical solution using numerical methods, [42-45]. The FEA method is the most accurate among many mathematical methods, [46-49]. ANSYS (Version 2020 R2) was used in this study as a representation of the finite element method. Figure 2 shows the three-dimensional model of the FG system created using SOLID186 and the eight-node fine grid size. Equations (8,9) are used in the FE simulation to get the properties of porous metal materials, then the resulting data is inserted into the model examined using Excel 2019. The mesh refinement was studied for convergence to make the numerical result as fine as possible with further mesh refinement [50-52]. Each plate side is subjected to boundary conditions. Based on modal analysis, the frequency parameters in the FGM sandwich panel structure are calculated, and the natural frequency at which stability can be determined.

a)

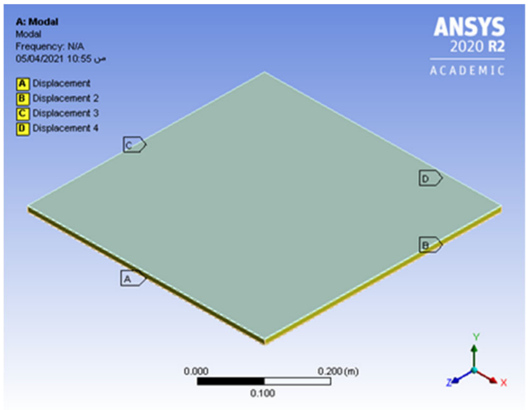

b)

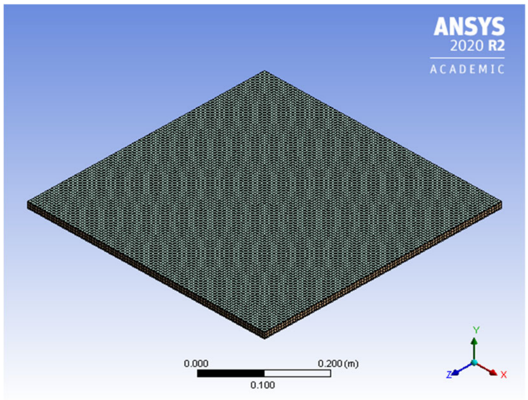

Fig. 2. Simulation of the sandwich plate using Ansys model: a) plate modelling, b) plate mesh

5. Experimental study

5.1. Specimen manufacturing

3D printing is a modern manufacturing technology that uses an additional process. This technique uses CAD software or a scan of a physical object to produce a three-dimensional model of an element. In medical technology, polylactic acid (PLA) is a leading biomaterial, and it is replacing petrochemical-based polymers due to its features. To describe the distribution pattern, the PLA samples with porosity are designed using the Solid Works program, then save the required model's geometry as a (.stl) file, and then use it to manufacture the sample through the CR-10 Max 3D printer as shown in Figure 3. Aluminium alloy (AA6061-T6) plate with a thickness of 0.5 mm was used for the face sheet, specified as highly suitable for multiple technical and aviation structural applications. The top and bottom surfaces of the face sheet were bonded to the FG core using Epoxy adhesive as shown in Figure 3. The material properties of the FG core and the face sheet are shown in Table 1 [53]. The face sheet is bonded to the FG core at the top and bottom surfaces using extraordinary adhesion (Epoxy), as shown in Figure 4.

a)

b)

Fig. 3. manufacturing FG specimens using 3D printing; a) 3D printing process, b) porous core production

Table 1.
Material properties employed in the FG sandwich

Property	FG core (PLA)	Face Sheets (Aluminium)
E (GPa)	2.4	70
ρ (kg/m^3)	1360	2702
μ	0.38	0.3

Fig. 4. FG sandwich plate specimens

5.2. Experimental setup and procedure

The fundamental natural frequency of sandwich plates with functionally graded porous metal can be measured by conducting free vibration experiments. A vibration test bench was designed and manufactured to perform modal analysis methods to find the sandwich panel's characteristics with an FGM core. The test specimens were made of FGM with a (300*300) mm cross-section with various core heights (5, 10, 15, 20, and 25) mm. The plate is attached to the fixtures, and the experiment is conducted based on simply boundary conditions. The electronic unit includes a data acquisition device (DAQ NI-6009) with two accelerometers ADXL type attached on the different positions on the upper and lower facing of the FGM sandwich plate with the aid of paraffin wax. A load cell type S with a digital weighing indicator (SI 4010) is used to calibrate the exiting force resulting from the impact.

Computer PC included the LabVIEW, and SIGVIEW software is used for free vibration measurements. The connections of DAQ, accelerometer, Impact hammer are as shown in Figure 5. A Piezoelectric IH-01 impulse force hammer model (IH-01) impact force instantaneously activates the sandwich plate specimen, generating an electrical signal according to the impact force, which is allowed to oscillate freely from there. Data acquisition NI-6009 sends the signals from sensors and stimulating hammer to a PC, which interferes with LabVIEW software.

Microsoft Excel 2019 was then used to display the results. Signals are converted from the time domain to the frequency domain with SIGVIEW software using Fast Fourier Transform (FFT), [45]. Experimental results obtain natural frequencies, and excitation frequencies closer to natural frequency are considered resonance conditions. The values of acceleration amplitude measured by using an accelerometer could be used to calculate logarithmic decrement. The damping ratio (ξ) is determined using the logarithmic decrement method depending on the modal signal, which is obtained experimentally by using the equation [54],

$$\delta = ln\,\frac{X_1}{X_2} = \frac{2\pi\zeta}{\sqrt{1-\zeta^2}} \tag{20}$$

where δ is the logarithmic decrement, X_1 and X_2 are any two consecutive acceleration amplitudes. Using modal analysis, the natural frequency of plate construction with different parameters was calculated. Therefore, the numerical results are compared by analytical results, evaluated by a solution for general equation of motion for plate structure, estimate the discrepancy for results calculated, [55-62], given the agreement for analytical solution suggesting a sandwich plate structure, with FGM core and porous effect. Then, the experimental results were calculated in comparison with other results calculated by analytical or numerical techniques to given the agreement for results were evaluated with various porous and plate parameters effect [63-70].

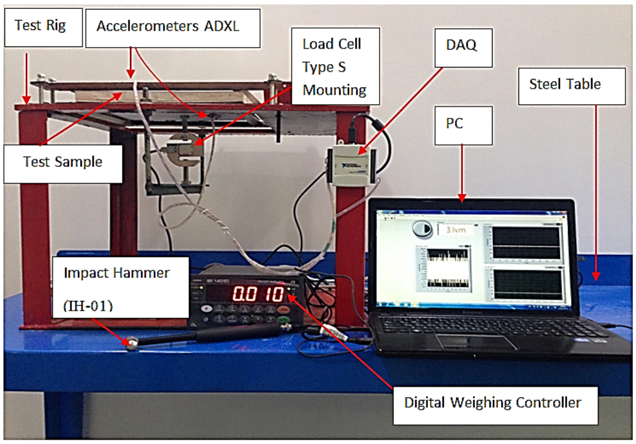

Fig. 5. Experimental setup for free vibration test

6. Results and discussion

In this work, an analytical investigation was carried out to analyse the FGM sandwich plate's free vibration problem with porous metal. The results calculated include the natural frequency and frequency parameter of the simply supported FGM sandwich plate with various parameters including porosity coefficient, face sheet thickness, aspect ratio, and gradient index. The materials are assumed to be homogenous at upper and lower plate parts, while the FGM part consists of one metal with a porosity gradient through-thickness direction. Numerical investigation using ANSYS software for verification purposes is also employed. The experimental program is achieved to check the accuracy of both analytical and numerical solutions. Non-dimensionalizing fundamental frequencies are described by the following relation,

$$\psi = \frac{\omega L^2}{H}\sqrt{\frac{\rho_o}{E_0}} \tag{21}$$

where ω is the natural frequency ρ_0= 1 kg/m^3, E_0=1 GPa [9]. Experiential results of the free vibration test for FG sandwich specimens with core height of 15 mm, γ=0.5, r =1 have been shown in Figures 6-8, respectively; each figure includes the exciting load, modal signal, and corresponding FFT analysis. Also, the natural frequencies can be calculated numerically by ANSYS software and theoretically using Equation (19). Many experimental results can be obtained using the same procedure for various parameters such as core height, power-law index, and porosity parameters.

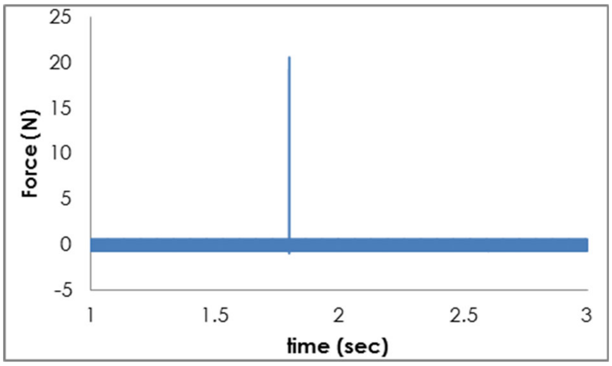

Fig. 6. Impulse load

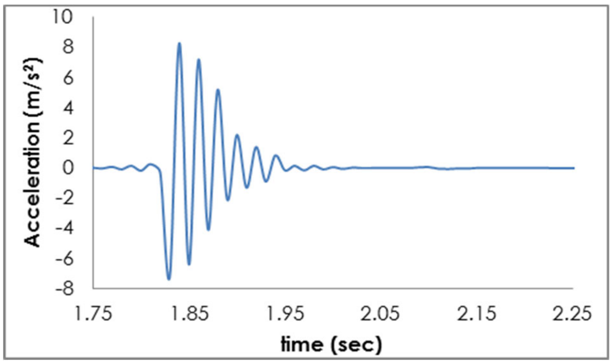

Fig. 7. Typical modal signal

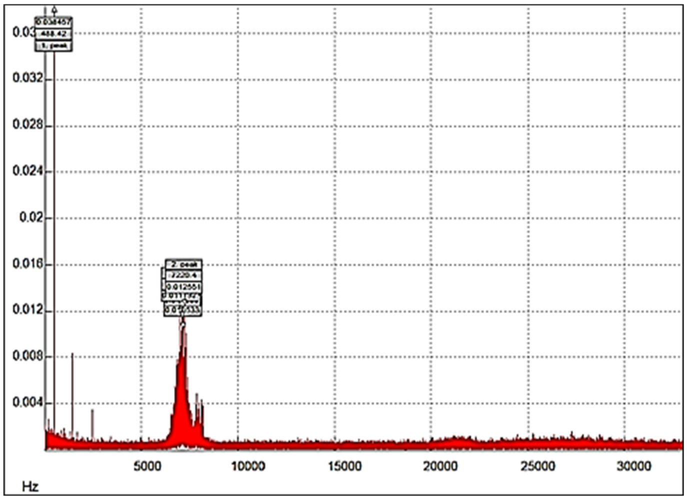

Fig. 8. Experimental results for (FFT)

Table 2.
The analytical, numerical, and experimental natural frequency values (Hz), γ =0.1 and 0.5 at r =1

h, mm	γ	Ana.	Num.	Exp.	Discrepancy analytical and numerical, %	Discrepancy analytical and experimental, %
5		285.07	286.81	253.89	0.61	10.94
10		427.56	429.24	398.44	0.39	6.81
15	0.1	544.40	546.09	488.42	0.31	10.28
20		648.77	650.68	592.58	0.29	8.66
25		745.74	743.21	682.66	0.34	8.46
5		307.44	309.23	269.73	0.57	12.27
10		465.76	464.12	395.42	0.35	15.10
15	0.5	594.02	596.09	524.77	0.35	11.66
20		707.32	710.37	667.89	0.43	5.57
25		811.59	809.84	751.11	0.22	7.45

Table 2 compares the analytical, numerical, and experimental results of the first natural frequency with two porosity parameters (γ = 0.1 and 0.5) and the gradient index (r =1) for different core heights (ranging from 5 to 25 mm). It can be concluded that the natural frequencies decrease with increasing gradient index and increase the porous parameter due to the decrease in the material rigidity. The results show that when the plate thickness increases and at higher mode frequencies, the CPT error percentage will be higher. There is an acceptable error between the analytical and numerical solutions with a maximum discrepancy of 0.576% with a slenderness ratio (a/h =100). While the maximum discrepancy reaches 15.103% between experimental and numerical results, it occurred at the same slenderness ratio. This percentage is affected by the power-law index and porous factor for the same FG plate thickness.

The maximum discrepancy between analytical and experimental results was 10.94% at a porosity ratio (γ = 0.5), As can be seen, there is suitable consistency between the proposed analytical solution and that is obtained by experiments. Figure 9 shows the numerical results of the surface response of a simply-supported sandwich plate. The variations in fundamental frequency at porosity (γ = 0) for different power-law indices (r = 0 to 0.5) and a face sheet thickness of 2 mm versus the core heights are given. Similarly, Figure 10 shows the same representation at porosity (γ = 0.25). It is found that the porosity ratio plays an important role in identifying free vibration frequency.

Depending on the modal signal obtained by frequent experiments as shown in Figure 8 and using Equation 21, the experimental results of the damping ratio for different core heights are given in Table 3. This table indicates a significant increase in damping ratio values with increasing core height and porosity for the same power-law index. frequencies due to the power-law index (r =50,100) were found. An excellent agreement can be observed with a difference of up to 8%, and this percentage is affected by the power-law index and porous factor for the same FG plate thickness. Figure 10 shows the numerical results of the surface response of a simply-supported sandwich plate. The variations in fundamental frequency at porosity (γ =0.25) for different power-law indices (r =0 to 0.5) and face sheet thickness 2 mm versus the core heights are given. It is noticed from the figures that the fundamental frequency values are reduced with the increase of the power-law index while the change of the porosity ratio is reversed.

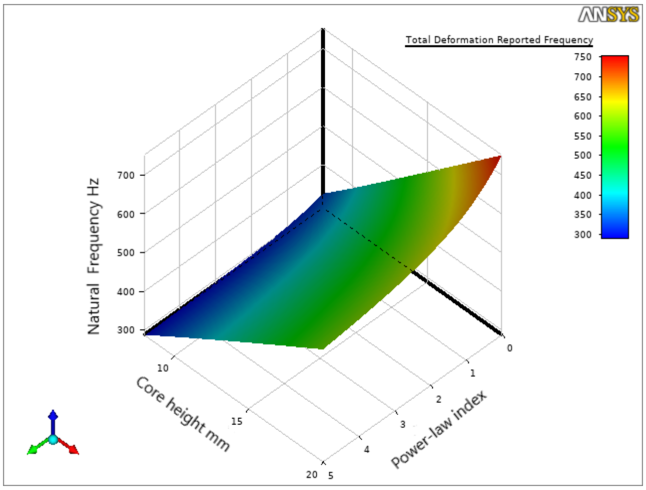

Fig. 9. Surface response at Porosity 0

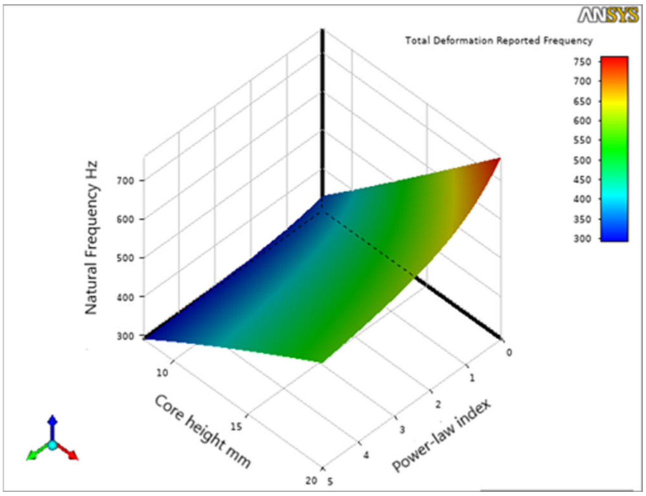

Fig. 10. Surface response at Porosity 0.25

Table 3.
The experimental results of the damping ratio

Porosity, %	Core height, mm	Power-law index, r	Damping ratio
10	10	1	0.0286
	15	1	0.0311
	20	1	0.0389
20	10	1	0.0255
	15	1	0.0292
	20	1	0.0348
30	10	1	0.0225
	15	1	0.0277
	20	1	0.0330

The numerical results of the frequency parameter for the imperfect FG sandwich plates with various porous factors with PLA core with an aspect ratio (a/h =50, a=b, skin thickness of 2.0 mm,) under the effect of seven types of boundary conditions are also presented in Table 4. The effect of porous factor and gradient index is studied. The value of the frequency parameter was found to increase with the number of constraints of the selected model; for example, in the CCCC model, the frequency parameter at porous factor (γ =0.3) and with gradient index (r =0.5) is (7.932), while in CCCS it was (7.279), in CSCS it was (4.273), in SSSS it was 6.104, and in FSFS it was (3.215).In contrast, for the CCCF boundary condition, the frequency parameter became (4.566). As boundaries become more constrained from SFSF to CCCC, higher fundamental frequencies result. Changing boundary constraints affect stiffness, explaining this behavior. In other words, the SFSF sandwich plate possesses the lowest nondimensional natural frequency among those of SSSS, SCSC, and CCCC composite plates, whereas the CCCC porous FG sandwich plate possesses the highest nondimensional natural frequency.

Table 5 gives results obtained by the analytical solution and FEA of the non-dimensional frequency of rectangular sandwich plates with FG Polyethylene core, (FG core thickness of 12 mm) with various porosity factors (γ= 0.1, 0.2, 0.3, 0.4 and 0.5), volume fraction index (r = 0, 0.5, 1, 2, 5, 10, 50 and 100) and by using four values of aspect ratio (a/b = 0.25, 0.5, 0.75, and 1). It can also be seen that the natural frequencies decrease with increasing gradient index and increase the porous parameter due to the decrease in the material rigidity. There is no remarkable difference between the natural frequencies due to the power-law index (r = 50, 100) was found. The impact of the porosity, geometrical, and volume fraction parameters of the plate on the free vibration of the porous sandwich plates is significant with the change in aspect ratio from 0.25 to 1.

Table 4.
Numerical results of the frequency parameter of square plates with PLA core (a/h =50), for different boundary conditions

B.Cs	Porosity Factor, γ	Power-law index, r								
		0	0.5	1	2	5	10	25	50	100
CCCC	0	7.317	7.317	7.317	7.317	7.317	7.317	7.317	7.317	7.317
	0.1	7.642	7.639	7.605	7.574	7.448	7.461	7.419	7.408	7.404
	0.2	7.731	7.815	7.623	7.683	7.572	7.491	7.469	7.458	7.449
	0.3	7.946	7.932	7.747	7.772	7.661	7.573	7.496	7.476	7.468
	0.4	8.269	8.016	7.825	7.785	7.743	7.687	7.581	7.544	7.522
	0.5	8.454	8.134	8.055	7.954	7.809	7.782	7.656	7.629	7.618
CCCS	0	6.646	6.646	6.646	6.646	6.646	6.646	6.646	6.646	6.646
	0.1	6.980	6.908	6.886	6.845	6.807	6.781	6.745	6.693	6.658
	0.2	7.265	7.182	7.144	7.062	6.990	6.955	6.889	6.770	6.684
	0.3	7.315	7.279	7.206	7.185	7.119	7.078	6.955	6.916	6.854
	0.4	7.450	7.395	7.350	7.292	7.199	7.096	6.987	6.956	6.917
	0.5	7.609	7.587	7.549	7.433	7.362	7.274	7.175	7.079	6.976
CSCS	0	6.295	6.295	6.295	6.295	6.295	6.295	6.295	6.295	6.295
	0.1	6.561	6.498	6.469	6.428	6.406	6.389	6.379	6.354	6.319
	0.2	6.785	6.735	6.687	6.621	6.594	6.567	6.517	6.491	6.394
	0.3	6.927	6.887	6.840	6.786	6.742	6.701	6.689	6.651	6.585
	0.4	7.118	7.027	6.997	6.881	6.845	6.788	6.736	6.712	6.664
	0.5	7.323	7.266	7.179	7.009	6.984	6.939	6.894	6.885	6.754
SSSS	0	5.672	5.672	5.672	5.672	5.672	5.672	5.672	5.672	5.672
	0.1	5.832	5.792	5.775	5.759	5.728	5.715	5.703	5.694	5.684
	0.2	6.129	6.066	5.975	5.845	5.818	5.775	5.734	5.727	5.698
	0.3	6.212	6.104	6.085	6.019	5.977	5.951	5.911	5.856	5.835
	0.4	6.475	6.435	6.408	6.385	6.277	6.193	6.165	6.072	5.987
	0.5	6.640	6.616	6.592	6.487	6.422	6.388	6.269	6.190	6.079
FCFC	0	3.805	3.805	3.805	3.805	3.805	3.805	3.805	3.805	3.805
	0.1	3.997	3.974	3.967	3.945	3.926	3.911	3.896	3.855	3.823
	0.2	4.168	4.106	3.998	3.976	3.968	3.942	3.916	3.895	3.864
	0.3	4.344	4.273	4.187	4.010	3.989	3.960	3.945	3.917	3.886
	0.4	4.435	4.376	4.225	4.164	4.055	3.987	3.967	3.938	3.904
	0.5	4.696	4.485	4.379	4.291	4.114	4.015	3.994	4.975	4.935
FSFS	0	2.838	2.838	2.838	2.838	2.838	2.838	2.838	2.838	2.838
	0.1	3.137	3.081	2.991	2.978	2.932	2.917	2.896	2.870	2.852
	0.2	3.222	3.185	3.079	3.004	2.989	2.967	2.926	2.900	2.883
	0.3	3.359	3.215	3.178	3.095	3.026	2.989	2.969	2.945	2.906
	0.4	3.436	3.389	3.226	3.103	2.077	3.002	2.995	2.976	2.934
	0.5	3.710	3.556	3.445	3.287	3.164	3.087	3.005	2.992	2.970
CCCF	0	3.750	3.750	3.750	3.750	3.750	3.750	3.750	3.750	3.750
	0.1	4.325	4.288	4.175	4.074	3.978	4.945	4.909	3.825	3.789
	0.2	4.519	4.458	4.317	4.270	4.116	4.086	3.996	3.964	3.854
	0.3	4.685	4.566	4.474	4.338	4.272	4.149	4.090	3.989	3.927
	0.4	4.825	4.775	4.657	4.496	4.370	4.244	4.176	4.082	3.980
	0.5	4.995	4.866	4.779	4.670	4.493	4.335	4.244	4.167	4.079

Table 5.
Analytical and Numerical results of the frequency of the rectangular plate with Polyethylene core height 12 mm

a/b	*r*	Porosity factor									
		0.1		0.2		0.3		0.4		0.5	
		Ana.	Num.	Ana.	Num.	Ana.	Num.	Ana.	Num.	Ana.	Num.
0.25	0	3.217	3.250	3.305	3.309	3.402	3.399	3.509	3.538	3.625	3.631
	0.5	3.189	3.193	3.245	3.288	3.305	3.377	3.370	3.486	3.436	3.517
	1	3.176	3.172	3.216	3.256	3.260	3.327	3.306	3.400	3.353	3.409
	2	3.161	3.160	3.188	3.238	3.216	3.277	3.245	3.302	3.274	3.375
	5	3.148	3.140	3.161	3.198	3.174	3.198	3.188	3.254	3.201	3.289
	10	3.142	3.134	3.149	3.162	3.156	3.174	3.163	3.198	3.171	3.219
	50	3.136	3.125	3.138	3.151	3.140	3.157	3.142	3.166	3.142	3.189
	100	3.135	3.117	3.136	3.145	3.137	3.143	3.138	3.145	3.140	3.167
0.5	0	3.784	3.779	3.885	3.835	4.002	4.108	4.127	4.139	4.264	4.213
	0.5	3.751	3.748	3.818	3.801	3.889	3.953	3.963	4.101	4.043	4.111
	1	3.735	3.722	3.784	3.792	3.835	3.888	3.889	3.947	3.944	3.938
	2	3.719	3.706	3.751	3.783	3.784	3.767	3.817	3.880	3.852	3.868
	5	3.703	3.696	3.719	3.708	3.734	3.744	3.750	3.853	3.766	3.757
	10	3.696	3.677	3.704	3.692	3.713	3.709	3.722	3.787	3.730	3.749
	50	3.690	3.657	3.692	3.688	3.693	3.695	3.695	3.746	3.697	3.729
	100	3.689	3.649	3.690	3.680	3.691	3.685	3.691	3.706	3.693	3.709
0.75	0	4.730	4.754	4.861	4.859	5.003	5.258	5.158	5.079	5.330	5.416
	0.5	4.689	4.712	4.773	4.806	4.861	5.079	4.954	4.846	5.054	5.226
	1	4.669	4.698	4.730	4.799	4.794	4.889	4.861	4.774	4.930	5.010
	2	4.649	4.672	4.689	4.751	4.730	4.781	4.772	4.701	4.815	4.864
	5	4.629	4.643	4.648	4.703	4.668	4.683	4.688	4.696	4.708	4.765
	10	4.620	4.607	4.631	4.684	4.641	4.667	4.651	4.676	4.662	4.732
	50	4.612	4.589	4.614	4.659	4.617	4.634	4.619	4.629	4.621	4.675
	100	4.611	4.573	4.612	4.624	4.613	4.623	4.614	4.599	4.615	4.651
1	0	6.055	6.129	6.221	6.339	6.403	6.5542	6.603	6.629	6.823	6.800
	0.5	6.002	6.105	6.109	6.299	6.222	6.4847	6.342	6.385	6.469	6.503
	1	5.976	5.946	6.055	6.188	6.136	6.3600	6.221	6.255	6.310	6.401
	2	5.950	5.876	6.001	6.104	6.054	6.136	6.108	6.191	6.163	6.189
	5	5.925	5.816	5.949	5.879	5.975	6.0805	6.000	6.008	6.026	6.089
	10	5.914	5.799	5.927	5.857	5.940	5.986	5.954	5.988	5.968	5.959
	50	5.904	5.754	5.906	5.842	5.909	5.9310	5.912	5.962	5.915	5.922
	100	5.902	5.712	5.904	5.803	5.905	5.911	5.906	5.937	5.908	5.117

From the obtained results, it is found that the porosity coefficients, gradient indices, and geometrical properties all have pronounced influences on the performance and reliability of the FG sandwich structures.

Figure 11 shows the frequency parameter at slenderness ratio (a/h=50) and face thickness of 2.0 mm for various porous metals (PEEK 30% CF, PEEK 30% GF, Polyethylene, PLA, Polystyrene, and Polyurethane foam).

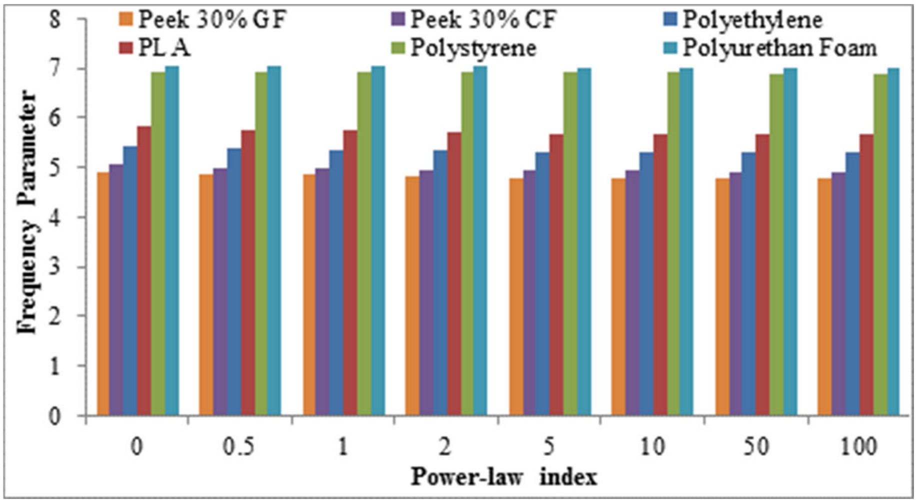

Fig. 11. Analytical results of frequency parameters with various core materials

It is concluded that polyurethane foam has higher stiffness than all other types, due to its high mechanical properties. This explains why this type is used in wide applications in construction and industrial applications. Table 6 gives the material properties of the various FG core constituents mentioned in this investigation [45].

Table 6.
Materials properties of the various FG core types used in numerical simulation

FG core type	E, MPa	ρ, kg/m^3	μ
Polyethylene	1100	950	0.42
Peek – 30 % CF	7700	1410	0.44
Peek – 30 % GF	6300	1510	0.34
Polyurethane foam	7.5	60	0
Polystyrene	3.0	100	0

7. Conclusions

The free vibration of a sandwich plate composed of an FG core and two isotropic panels is studied. The governing equation is derived using the linear constitutive relationship of the plate based on CPT. The material properties are calculated according to the suggested mixing rules. A comprehensive comparative study was carried out with numerical and experimental techniques to verify the accuracy of the analytical solution. The complete numerical results are introduced, including fundamental natural frequencies expressed in essential parameters such as power-law index, porosity coefficient, slenderness ratio, and boundary conditions. The current work's main conclusions are described as,

1. The proposed analytical method is an efficient tool for characterizing the natural frequencies of sandwich structures with porous FG cores based on numerous criteria.
2. Both analytical and experimental experiments have shown that natural frequencies increase with increasing porosity factors and decrease with increasing gradient indices.
3. As can be seen from the results of the table and graph, there is a direct correlation between aspect ratio (a/b) and slenderness ratio (a/h), as well as porosity distributions, when examining free vibration properties of rectangular sandwich plates.
4. Changing the core surface height from (0.005 m) to (0.025 m) increases the analytical natural frequency by 504.143 Hz at 10% porosity ratio (r =1), while at porosity ratio (γ = 50%) and power-law index (r =1), the increase will be 460.67 Hz.
5. Several factors influence the reliability of the observed natural frequency, most significantly noise and deviations in frequency response, that impact the validity of the experimental results.

Acknowledgements

The authors are thankful to the Mechanical Department of the University of Technology, and the University of Kufa, Faculty of Engineering, Iraq.

References

[1] E.K. Njim, M. Al-Waily, S. H. Bakhy, A Critical Review of Recent Research of Free Vibration and Stability of Functionally Graded Materials of Sandwich Plate, IOP Conference Series: Materials Science and Engineering 1094 (2021) 012081. DOI: https://doi.org/10.1088/1757-899X/1094/1/012081

[2] B. Saleh, J. Jiang, R. Fathi, T. Al-hababi, Q. Xu, L. Wang, D. Song, A. Ma, 30 Years of functionally graded materials: An overview of manufacturing methods, Applications, and Future Challenges, Composites Part B: Engineering 201 (2020) 108376. DOI: https://doi.org/10.1016/j.compositesb.2020.108376

[3] A. Garg, M.O. Belarbi, H.D. Chalak, A. Chakrabarti, A review of the analysis of sandwich FGM structures, Composite Structures 258 (2021) 113427. DOI: https://doi.org/10.1016/j.compstruct.2020.113427

[4] E.K. Njim, S.H. Bakhy, M. Al-Waily, Analytical and numerical investigation of buckling load of functionally graded materials with porous metal of sandwich plate, Materials Today: Proceedings (2021) (available online). DOI: https://doi.org/10.1016/j.matpr.2021.03.557

[5] Y.H. Dong, Y.H. Li, D. Chen, J. Yang, Vibration characteristics of functionally graded graphene reinforced porous nanocomposite cylindrical shells with spinning motion, Composites Part B: Engineering 145 (2018) 1-13. DOI: https://doi.org/10.1016/j.compositesb.2018.03.009

[6] A.M. Zenkour, A quasi-3D refined theory for functionally graded single-layered and sandwich plates with porosities, Composite Structures 201 (2018) 38-48. DOI: https://doi.org/10.1016/j.compstruct.2018.05.147

[7] M. Arefi, F. Najafitabar, Buckling and free vibration analyses of a sandwich beam made of a soft core with FG-GNPs reinforced composite face-sheets using Ritz Method, Thin-Walled Structures 158 (2021) 107200. DOI: https://doi.org/10.1016/j.tws.2020.107200

[8] M.D. Sciuva, M. Sorrenti, Bending, free vibration, and buckling of functionally graded carbon nanotube-reinforced sandwich plates, using the extended Refined Zigzag Theory, Composite Structures 227 (2019) 111324. DOI: https://doi.org/10.1016/j.compstruct.2019.111324

[9] M. Amirpour, S. Bickerton, E. Calius, B.R. Mace, R. Das, Numerical and experimental study on free vibration of 3D-printed polymeric functionally graded plates, Composite Structures 189 (2018) 192-205. DOI: https://doi.org/10.1016/j.compstruct.2018.01.056

[10] N. Wattanasakulpong, V. Ungbhakorn, Linear and nonlinear vibration analysis of elastically restrained ends FGM beams with porosities, Aerospace Science and Technology 32/1 (2014) 111-120. DOI: https://doi.org/10.1016/j.ast.2013.12.002

[11] N. Wattanasakulpong, A. Chaikittiratana, Flexural vibration of imperfect functionally graded beams based on Timoshenko beam theory, Chebyshev collocation method, Meccanica 50 (2015) 1331-1342. DOI: https://doi.org/10.1007/s11012-014-0094-8

[12] A. Muc, J. Flis, Flutter characteristics and free vibrations of rectangular functionally graded porous plates, Composite Structures 261 (2021) 113301. DOI: https://doi.org/10.1016/j.compstruct.2020.113301

[13] K. Xie, Y. Wang, H. Niu, H. Chen, Large-amplitude nonlinear free vibrations of functionally graded plates with porous imperfection: A novel approach based on energy balance method, Composite Structures 246 (2020) 112367. DOI: https://doi.org/10.1016/j.compstruct.2020.112367

[14] S. Hayat, S. Meriem, Vibration analysis of functionally graded plates with porosity composed of a mixture of Aluminum (Al) and Alumina (Al_2O_3) embedded in an elastic medium, Fracture and Structural Integrity 13/50 (2019) 286-299. DOI: https://doi.org/10.3221/IGF-ESIS.50.24

[15] X.Y. Zhang, G. Fang, S. Leeflang, A.A. Zadpoor, J. Zhou, Topological design, permeability, and mechanical behavior of additively manufactured functionally graded porous metallic biomaterials, Acta Biomaterialia 84 (2018) 437-452. DOI: https://doi.org/10.1016/j.actbio.2018.12.013

[16] A.H. Mostefa, M. Slimane, Influence of porosity on the analysis of sandwich plates FGM using of high order shear deformation theory, Fracture and Structural Integrity 14/51 (2020) 199-214. DOI: https://doi.org/10.3221/IGF-ESIS.51.16

[17] S.J. Singh, S.P. Harsha, Analysis of porosity effect on free vibration and buckling responses for sandwich sigmoid function based functionally graded material plate resting on Pasternak foundation using Galerkin Vlasov's method, Journal of Sandwich Structures and Materials 23/5 (2021) 1717-1760. DOI: https://doi.org/10.1177/1099636220904340

[18] V. Kumar, S.J. Singh, V.H. Saran, S.P. Harsha, Vibration characteristics of porous FGM plate with

variable thickness resting on Pasternak's foundation, European Journal of Mechanics-A/Solids 85 (2021) 104124.
DOI: https://doi.org/10.1016/j.euromechsol.2020.104124

[19] T. Khan, O.A. Aydın, V. Acar, M.R. Aydın, B. Hülagü, H. Bayrakçeken, M.Ö. Seydibeyoğlu, H. Akbulut, Experimental investigation of mechanical and modal properties of Al_2O_3 nanoparticle reinforced polyurethane core sandwich structures, Materials Today Communications 24 (2020) 101233. DOI: https://doi.org/10.1016/j.mtcomm.2020.101233

[20] M. Kaddari, A. Kaci, A.A. Bousahla, A. Tounsi, F. Bourada, A. Tounsi, E.A. Bedia, M.A. Al-Osta, A study on the structural behavior of functionally graded porous plates on elastic foundation using a new quasi-3D model: bending and free vibration analysis, Computers and Concrete 25/1 (2020) 37-57.
DOI: https://doi.org/10.12989/cac.2020.25.1.037

[21] Q. Li, D. Wu, X. Chen, L. Liu, Y. Yu, W. Gao, Nonlinear vibration and dynamic buckling analyses of sandwich functionally graded porous plate with graphene platelet reinforcement resting on Winkler–Pasternak elastic foundation, International Journal of Mechanical Sciences 148 (2018) 596-610. DOI: https://doi.org/10.1016/j.ijmecsci.2018.09.020

[22] Y. Xue, G. Jin, X. Ma, H. Chen, T. Ye, M. Chen, Y. Zheng, Free vibration analysis of porous plates with porosity distributions in the thickness and in-plane directions using isogeometric approach, International Journal of Mechanical Sciences 152 (2019) 346-362. DOI: https://doi.org/10.1016/j.ijmecsci.2019.01.004

[23] M. Abderrahmane, K. Abdelhakim, A.B. Abdelmoumen, B. Fouad, T. Abdeldjebbar, H.B. Kouider, T. Abdelouahed, E.A. Adda Bedia, S.R. Mahmoud, A four-unknown refined plate theory for dynamic analysis of FG-sandwich plates under various boundary conditions, Steel and Composite Structures 36/3 (2020) 355-367.
DOI: https://doi.org/10.12989/scs.2020.36.3.355

[24] C. Li, H.S. Shen, H. Wang, Z. Yu, Large amplitude vibration of sandwich plates with functionally graded auxetic 3D lattice core, International Journal of Mechanical Sciences 174 (2020) 105472.
DOI: https://doi.org/10.1016/j.ijmecsci.2020.105472

[25] S. Brischetto, Hygrothermoelastic analysis of multi-layered composite and sandwich shells, Journal of Sandwich Structures and Materials 15/2 (2013) 168-202. DOI: https://doi.org/10.1177/1099636212471358

[26] A. Garg, H.D. Chalak, A review on analysis of laminated composite and sandwich structures under hygrothermal conditions, Thin-Walled Structures 142 (2019) 205-226.
DOI: https://doi.org/10.1016/j.tws.2019.05.005

[27] A. Garg, H.D. Chalak, Analysis of non-skew and skew laminated composite and sandwich plates under hygro-thermomechanical conditions including transverse stress variations, Journal of Sandwich Structures and Materials 23/8 (2021) 3471-3494.
DOI: https://doi.org/10.1177/1099636220932782

[28] H. Krishna, H.D. Chalak, Behaviour of laminated composite sandwiched structures under thermal conditions, IOP Conference Series: Materials Science and Engineering 872 (2020) 012148. DOI: https://doi.org/10.1088/1757-899X/872/1/012148

[29] R. Kumar, A. Lal, B.M. Sutaria, Non-linear deflection and stress analysis of laminated composite sandwich plate with elliptical cutout under different transverse loadings in hygro-thermal environment, Curved and Layered Structures 7/1 (2020) 80-100.
DOI: https://doi.org/10.1515/cls-2020-0008

[30] A. Garg, H.D. Chalak, M.O. Belarbi, A. Chakrabarti, M.S.A. Houari, Finite Element-based Free Vibration Analysis of Power-Law, Exponential and Sigmoidal Functionally Graded Sandwich Beams, Journal of The Institution of Engineers (India): Series C 102 (2021) 1167-1201.
DOI: https://doi.org/10.1007/s40032-021-00740-5

[31] H. Hirane, M.O. Belarbi, M.S.A. Houari, A. Tounsi, On the layerwise finite element formulation for static and free vibration analysis of functionally graded sandwich plates, Engineering with Computers (2021) (published online). DOI: https://doi.org/10.1007/s00366-020-01250-1

[32] P.V. Vinh, A. Tounsi, The role of spatial variation of the nonlocal parameter on the free vibration of functionally graded sandwich nanoplates. Engineering with Computers (2021) (published online). DOI: https://doi.org/10.1007/s00366-021-01475-8

[33] P.V. Vinh, L.Q. Huy, Finite element analysis of functionally graded sandwich plates with porosity via a new hyperbolic shear deformation theory, Defence Technology (2021) (available online).
DOI: https://doi.org/10.1016/j.dt.2021.03.006

[34] P.V. Vinh, Analysis of bi-directional functionally graded sandwich plates via higher-order shear deformation theory and finite element method, Journal

of Sandwich Structures & Materials (2021) (published online).
DOI: https://doi.org/10.1177/10996362211025811

[35] S.H. Chi, Y.L. Chung, Mechanical behavior of functionally graded material plates under transverse load Part I: Analysis, International Journal of Solids and Structures 43/13 (2006) 3657-3674. DOI: https://doi.org/10.1016/j.ijsolstr.2005.04.011

[36] M. Latifi, F. Farhatnia, M. Kadkhodaei, Buckling analysis of rectangular functionally graded plates under various edge conditions using Fourier series expansion, Europe a Journal of Mechanics-A/Solids 41 (2013) 16-27.
DOI: https://doi.org/10.1016/j.euromechsol.2013.01.008

[37] M.A. Al-Shammari, M. Al-Waily, Theoretical and Numerical Vibration Investigation Study of Orthotropic Hyper Composite Plate Structure, International Journal of Mechanical and Mechatronics Engineering 14/6 (2014) 1-21.

[38] M. Al-Waily, K.K. Resan, A.H. Al-Wazir, Z.A.A. Abud Ali, Influences of Glass and Carbon Powder Reinforcement on the Vibration Response and Characterization of an Isotropic Hyper Composite Materials Plate Structure, International Journal of Mechanical and Mechatronics Engineering 17/6 (2017) 74-85.

[39] K.J. Jweeg, A.S. Hammood, M. Al-Waily, A Suggested Analytical Solution of Isotropic Composite Plate with Crack Effect, International Journal of Mechanical and Mechatronics Engineering 12/5 (2012) 44-58.

[40] A.A. Alhumdany, M. Al-Waily, M.H.K. Al-Jabery, Theoretical and Experimental Investigation of Using Date Palm Nuts Powder into Mechanical Properties and Fundamental Natural Frequencies of Hyper Composite Plate, International Journal of Mechanical and Mechatronics Engineering 16/1 (2016) 70-80.

[41] E.N. Abbas, M.J. Jweeg, M. Al-Waily, Analytical and Numerical Investigations for Dynamic Response of Composite Plates Under Various Dynamic Loading with the Influence of Carbon Multi-Wall Tube Nano Materials, International Journal of Mechanical and Mechatronics Engineering 18/6 (2018) 1-10.

[42] M.J. Jweeg, M. Al-Waily, A.A. Deli, Theoretical and Numerical Investigation of Buckling of Orthotropic Hyper Composite Plates, International Journal of Mechanical and Mechatronics Engineering 15/4 (2015) 1-12.

[43] J.S. Chiad, M. Al-Waily, M.A. Al-Shammari, Buckling Investigation of Isotropic Composite Plate Reinforced by Different Types of Powders, International Journal of Mechanical Engineering and Technology 9/9 (2018) 305-317.

[44] M. Al-Waily, M.A. Al-Shammari, M.J. Jweeg, An Analytical Investigation of Thermal Buckling Behavior of Composite Plates Reinforced by Carbon Nano Particles, Engineering Journal 24/3 (2020) 11-21. DOI: https://doi.org/10.4186/ej.2020.24.3.11

[45] E.K. Njim, M. Al-Waily, S.H. Bakhy, A Review of the Recent Research on the Experimental Tests of Functionally Graded Sandwich Panels, Journal of Mechanical Engineering Research and Developments 44/3 (2021) 420-441.

[46] M. Al-Waily, A.A. Deli, A.D. Al-Mawash, Z.A.A. Abud Ali, Effect of Natural Sisal Fiber Reinforcement on the Composite Plate Buckling Behavior, International Journal of Mechanical and Mechatronics Engineering 17/1 (2017) 30-37.

[47] V.N. Burlayenko, T. Sadowski, Free vibrations and static analysis of functionally graded sandwich plates with three-dimensional finite elements, Meccanica 55 (2020) 815-832.
DOI: https://doi.org/10.1007/s11012-019-01001-7

[48] S.E. Sadiq, M.J. Jweeg, S.H. Bakhy, The Effects of Honeycomb Parameters on Transient Response of an Aircraft Sandwich Panel Structure, IOP Conference Series: Materials Science and Engineering 928 (2020) 022126.
DOI: https://doi.org/10.1088/1757-899X/928/2/022126

[49] Z.A.A. Abud Ali, A.A. Kadhim, R.H. Al-Khayat, M. Al-Waily, Review Influence of Loads upon Delamination Buckling in Composite Structures, Journal of Mechanical Engineering Research and Developments 44/3 (2021) 392-406.

[50] M. Al-Waily, Z.A.A. Abud Ali, A Suggested Analytical Solution of Powder Reinforcement Effect on Buckling Load for Isotropic Mat and Short Hyper Composite Materials Plate, International Journal of Mechanical and Mechatronics Engineering 15/4 (2015) 80-95.

[51] M.R. Ismail, Z.A.A. Abud Ali, M. Al-Waily, Delamination Damage Effect on Buckling Behavior of Woven Reinforcement Composite Materials Plate, International Journal of Mechanical and Mechatronics Engineering 18/5 (2018) 83-93.

[52] E.K. Njim, S.H. Bakhy, M. Al-Waily, Optimization design of vibration characterizations for functionally graded porous metal sandwich plate structure, Materials Today: Proceedings (2021) (available online).
DOI: https://doi.org/10.1016/j.matpr.2021.03.235

[53] K.F. Arndt, M.D. Lechner, Polymer Solids and Polymer Melts–Mechanical and Thermomechanical Properties of Polymers, 1st Edition, Springer-Verlag Berlin Heidelberg, 2014.
DOI: https://doi.org/10.1007/978-3-642-55166-6

[54] L. Zheng, X.S. Huo, Y. Yuan, Experimental investigation on dynamic properties of rubberized concrete, Construction and Building Materials 22/5 (2008) 939-947.
DOI: https://doi.org/10.1016/j.conbuildmat.2007.03.005

[55] M.A. Al-Shammari, M. Al-Waily, Analytical Investigation of Buckling Behavior of Honeycombs Sandwich Combined Plate Structure, International Journal of Mechanical and Production Engineering Research and Development 8/4 (2018) 771-786.

[56] S.M. Abbas, K.K. Resan, A.K. Muhammad, M. Al-Waily, Mechanical and Fatigue Behaviors of Prosthetic for Partial Foot Amputation with Various Composite Materials Types Effect, International Journal of Mechanical Engineering and Technology 9/9 (2018) 1-8.

[57] H.J. Abbas, M.J. Jweeg, M. Al-Waily, A.A. Diwan, Experimental Testing and Theoretical Prediction of Fiber Optical Cable for Fault Detection and Identification, Journal of Engineering and Applied Sciences 14/2 (2019) 430-438.
DOI: http://dx.doi.org/10.36478/jeasci.2019.430.438

[58] E.N. Abbas, M. Al-Waily, T.M. Hammza, M.J. Jweeg, An Investigation to the Effects of Impact Strength on Laminated Notched Composites used in Prosthetic Sockets Manufacturing, IOP Conference Series: Materials Science and Engineering 928 (2020) 022081.
DOI: https://doi.org/10.1088/1757-899X/928/2/022081

[59] S.G. Hussein, M.A. Al-Shammari, A.M. Takhakh, M. Al-Waily, Effect of Heat Treatment on Mechanical and Vibration Properties for 6061 and 2024 Aluminum Alloys, Journal of Mechanical Engineering Research and Developments 43/1 (2020) 48-66.

[60] A.A. Kadhim, E.A. Abbod, A.K. Muhammad, K.K. Resan, M. Al-Waily, Manufacturing and Analyzing of a New Prosthetic Shank with Adapters by 3D Printer, Journal of Mechanical Engineering Research and Developments 44/3 (2021) 383-391.

[61] Q.H. Jebur, M.J. Jweeg, M. Al-Waily, H.Y. Ahmad, K.K. Resan, Hyperelastic models for the description and simulation of rubber subjected to large tensile loading, Archives of Materials Science and Engineering 108/2 (2021) 75-85.
DOI: https://doi.org/10.5604/01.3001.0015.0256

[62] E.K. Njim, S.H. Bakhy, M. Al-Waily, Analytical and Numerical Investigation of Buckling Behavior of Functionally Graded Sandwich Plate with Porous Core, Journal of Applied Science and Engineering 25/2 (2022) 339-347.
DOI: https://doi.org/10.6180/jase.202204_25(2).0010

[63] M.J. Jweeg, A.S. Hammood, M. Al-Waily, Experimental and Theoretical Studies of Mechanical Properties for Reinforcement Fiber Types of Composite Materials, International Journal of Mechanical and Mechatronics Engineering 12/4 (2012) 62-75.

[64] A.A. Kadhim, M. Al-Waily, Z.A.A. Abud Ali, M.J. Jweeg, K.K. Resan, Improvement Fatigue Life and Strength of Isotropic Hyper Composite Materials by Reinforcement with Different Powder Materials, International Journal of Mechanical and Mechatronics Engineering 18/2 (2018) 77-86.

[65] M.J. Jweeg, M. Al-Waily, A.K. Muhammad, K.K. Resan, Effects of Temperature on the Characterisation of a New Design for a Non-Articulated Prosthetic Foot, IOP Conference Series: Materials Science and Engineering 433 (2018) 012064.
DOI: https://doi.org/10.1088/1757-899X/433/1/012064

[66] E.N. Abbas, M.J. Jweeg, M. Al-Waily, Fatigue Characterization of Laminated Composites used in Prosthetic Sockets Manufacturing, Journal of Mechanical Engineering Research and Developments 43/5 (2020) 384-399.

[67] M. Al-Waily, M.H. Tolephih, M.J. Jweeg, Fatigue Characterization for Composite Materials used in Artificial Socket Prostheses with the Adding of Nanoparticles, IOP Conference Series: Materials Science and Engineering 928 (2020) 022107. DOI: https://doi.org/10.1088/1757-899X/928/2/022107

[68] E.K. Njim, S.H. Bakhy, M. Al-Waily, Analytical and Numerical Investigation of Free Vibration Behavior for Sandwich Plate with Functionally Graded Porous Metal Core, Pertanika Journal of Science and Technology 29/3 (2021) 1655-1682.
DOI: https://doi.org/10.47836/pjst.29.3.39

[69] N.D. Fahad, A.A. Kadhim, R.H. Al-Khayat, M. Al-Waily, Effect of SiO_2 and Al_2O_3 hybrid nano materials on fatigue behavior for laminated composite materials used to manufacture artificial socket prostheses, Materials Science Forum 1039 (2021) 493-509. DOI: https://doi.org/10.4028/www.scientific.net/MSF.1039.493

[70] Q.H. Jebur, M.J. Jweeg, M. Al-Waily, Ogden model for characterising and simulation of PPHR Rubber under different strain rates, Australian Journal of Mechanical Engineering (2021) (published online). DOI: https://doi.org/10.1080/14484846.2021.1918375